Rab14/MACF2 complex regulates endosomal targeting during cytokinesis

Paulius Gibieža[a], Eric Peterman[b], Huxley K. Hoffman[c], Schuyler Van Engeleburg[c], Vytenis Arvydas Skeberdis[a], and Rytis Prekeris[b,*]

[a]Laboratory of Cell Culture, Institute of Cardiology, Lithuanian University of Health Sciences, Kaunas LT-50162, Lithuania; [b]Department of Cell and Developmental Biology, University of Colorado Anschutz Medical, Campus, Aurora, CO 80045; [c]Department of Biological Sciences 20208, Denver University, Denver, CO

ABSTRACT **Abscission is a complex cellular process that is required for mitotic division. It is well established that coordinated and localized changes in actin and microtubule dynamics are vital for cytokinetic ring formation, as well as establishment of the abscission site. Actin cytoskeleton reorganization during abscission would not be possible without the interplay between Rab11- and Rab35-containing endosomes and their effector proteins, whose roles in regulating endocytic pathways at the cleavage furrow have now been studied extensively. Here, we identified Rab14 as a novel regulator of cytokinesis. We demonstrate that depletion of Rab14 causes either cytokinesis failure or significantly prolongs division time. We show that Rab14 contributes to the efficiency of recruiting Rab11-endosomes to the thin intracellular bridge (ICB) microtubules and that Rab14 knockout leads to inhibition of actin clearance at the abscission site. Finally, we demonstrate that Rab14 binds to microtubule minus-end interacting MACF2/CAMSAP3 complex and that this binding affects targeting of endosomes to the ICB microtubules. Collectively, our data identified Rab14 and MACF2/CAMSAP3 as proteins that regulate actin depolymerization and endosome targeting during cytokinesis.**

Monitoring Editor
Ahna Skop
University of Wisconsin, Madison

Received: Sep 23, 2020
Revised: Jan 29, 2021
Accepted: Feb 2, 2021

INTRODUCTION

Cytokinesis is the last stage of the cell cycle that leads to a physical separation of two daughter cells. Cytokinesis is initiated by a formation of cytokinetic actomyosin ring and contraction of this cytokinetic ring leaves two daughter cells connected with a thin intracellular bridge (ICB) that contains a microtubule-rich structure known as the midbody (MB) (Dionne *et al.*, 2015). The resolution of the ICB, the process known as abscission, is the last step of cell division. It has been demonstrated that abscission depends on coordinated changes in endocytic membrane traffic and cellular cytoskeleton, such as spastin-dependent cutting of ICB microtubules and depolymerization of actin cytoskeleton (Wilson *et al.*, 2005; Connell *et al.*, 2009; Guizetti *et al.*, 2011; Prekeris, 2011; Fremont *et al.*, 2017a). These localized changes in actin and microtubule cytoskeleton are vital to defining the abscission site and recruitment of ESCRT complex to regulating the timing of completing cell division (Schiel and Prekeris, 2010; Fremont *et al.*, 2017; Addi *et al.*, 2018; Vietri *et al.*, 2020).

While it is now well established that Rab11- and Rab35-containing endosomes are the key regulators of abscission (Dambournet *et al.*, 2011; Prekeris, 2011; Schiel and Prekeris, 2013), many questions remain. For example, it remains to be fully understood how these endosomes are targeted specifically to the ICB. Indeed, Rab11 and Fip3 (Rab11-effector protein) were shown to be associated with a specialized subpopulation of recycling endosomes that are delivered to the abscission site only at late telophase (Schiel *et al.*, 2012). Interestingly, during metaphase and anaphase Rab11/Fip3 associates with centrosomes (Collins *et al.*, 2012; Simon *et al.*, 2008), presumably preventing premature delivery of Rab11/Fip3-endosomes to the ICB. Furthermore, during early telophase, Rab11/Fip3-containing

This article was published online ahead of print in MBoC in Press (http://www.molbiolcell.org/cgi/doi/10.1091/mbc.E20-09-0607) on February 10, 2021.

Author contributions: R.P. and V.A.S. designed experiments and oversaw entire project; P.G. performed most of the time-lapse analyses as well as functional assays; P.G. also generated Rab14 KO and KD lines as well as MACF2 KD lines; E.P. performed MB proteomic analysis and performed some of the immunofluorescence analyses; H.K.H. and S.V.E. generated GFP-tagged endogenous Rab14 cell line.

Conflict of interest: the authors declare that they have no conflict of interest.

*Address correspondence to: Rytis Prekeris (rytis.prekeris@ucdenver.edu).

Abbreviations used: gRNA, guide RNA; HDRT, homology-directed repair template; ICB, intracellular bridge; KD, knockdown; KO, knockout; LatA, latrunculin A; MACF, microtubule actin cross-linking factor; MD, midbody; qPCR, quantitative PCR; RNP, ribonucleoprotein; ROI, region of interest.

© 2021 Gibieža *et al.* This article is distributed by The American Society for Cell Biology under license from the author(s). Two months after publication it is available to the public under an Attribution–Noncommercial–Share Alike 3.0 Unported Creative Commons License (http://creativecommons.org/licenses/by-nc-sa/3.0).

"ASCB®," "The American Society for Cell Biology®," and "Molecular Biology of the Cell®" are registered trademarks of The American Society for Cell Biology.

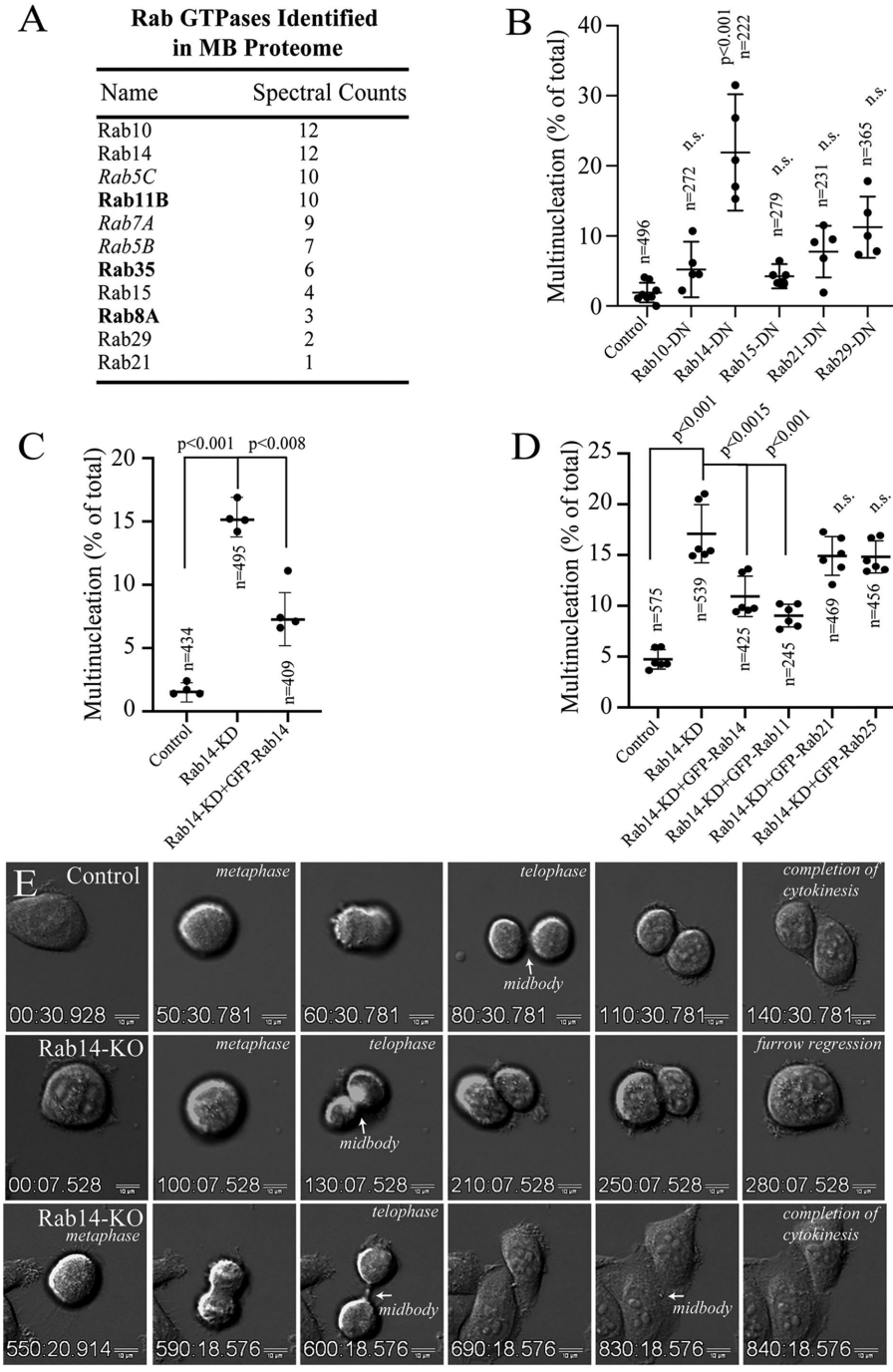

FIGURE 1: Rab14 is required for completion of cytokinesis. (A) Endocytic Rab GTPases present in postmitotic MB proteome. (B) HeLa cells were transfected with GFP-tagged dominant-negative mutants of various MB-associated Rabs. Multinucleated cells were then counted and expressed as the percentage of total number of cells. Data shown are the means and SD derived from several independent experiments represented by individual dots; *n* is the total number of cells counted. (C, D) Control and Rab14-KD cells were transfected with various GFP-tagged Rabs. The ability of overexpression to decrease multinucleation was then analyzed. Data shown are the means and SD derived from several independent experiments represented by individual dots; *n* is the total number of cells counted. (E) Individual images taken from time-lapse analysis of dividing control (top row) and Rab14-KO (both bottom rows) cells (also see Supplemental Movies S1–S3). Time units listed on the images are minutes.

endosomes leave centrosomes and translocate to minus-ends of ICB microtubules (Simon *et al.*, 2008; Schiel *et al.*, 2012). Although the functional consequence of this translocation remains to be fully defined, it could be hypothesized that this recruitment of endosomes to microtubule minus-ends is required for efficient delivery of Rab11/Fip3-endosomes to the ICB and the MB during abscission.

Since the roles of Rab11 and Rab35 in the control of cell division have been previously described, in this study we focus on identifying the possible functions of other Rabs in regulating the endosomal traffic to the abscission site during mitotic cell division. Recently we completed a proteomic analysis of postabscission MBs and have shown that postabscission MBs contain multiple endocytic Rabs (Peterman *et al.*, 2019). In this study we test all of these MB-associated endocytic Rabs for their requirement during cytokinesis. We show that, in addition to Rab11 and Rab35, Rab14 also is required for cytokinesis. We demonstrate that overexpression of Rab14 dominant-negative mutants, as well as knockdown (KD) or knockout (KO) of Rab14, causes multinucleation and an increase in time required for cells to divide. Also, we show that Rab14 affects Rab11/Fip3-endosomes targeting to the ICB and also appears to mediate cytokinesis via actin clearance from the ICB. Finally, using coimmunoprecipitation/proteomic analysis, we identified the microtubule-bundling MACF2 protein as Rab14 effector. Importantly, MACF2 KD leads to cytokinetic defects and also affects the recruitment of Rab14 as well as Rab11/Fip3-endosomes to the ICB. Thus, we propose that Rab14/MACF2 complex regulates cytokinesis, at least in part, via affecting Rab11/Fip3-endosome targeting to the ICB microtubules.

RESULTS

Rab14 regulates cytokinesis

Multiple studies have demonstrated that endocytic transport plays an important role in regulating abscission; specifically, endocytic Rab11a/b and Rab35 were implicated to mediate this process (Schiel *et al.*, 2013; Fremont and Echard 2018; Gibieza and Prekeris 2018). Since numerous Rab GTPases are known to regulate endocytic transport, we set out to identify other endocytic Rab GTPases that may contribute to cytokinesis. Recently, we completed proteomic analysis of MBs purified from HeLa cells (Peterman *et al.*, 2019), in which we first asked which Rab GTPases are present at the MBs and which could play a role in cell division. In total, we identified 11 endocytic MB-associated Rabs GTPases (Figure 1A) (Peterman *et al.*, 2019). Importantly, we identified Rab11b and Rab35, both known regulators of abscission (Fielding *et al.*, 2005; Kouranti *et al.*, 2006; Dambournet *et al.*, 2011; Collins *et al.*, 2012), as well as Rab8, which has also been shown to be

present in the ICB (Schiel *et al.,* 2012). Since Rab10, Rab14, Rab15, Rab21, and Rab29 have not been investigated for their involvement in regulating cell division, we next tested whether these Rabs may be required for completing cytokinesis. We have decided not to include Rab5 and Rab7 in this analysis since these two Rab GTPases regulate early endosome and lysosomal targeting; thus, their depletion could lead to wide-ranging defects and an indirect effect on cytokinesis.

All Rab GTPases in cells cycle between GTP-bound (active) and GDP-bound (inactive) states. Thus, to test the involvement of the prior identified Rab GTPases in cytokinesis, we created dominant-negative GFP-tagged Rab10, Rab14, Rab15, Rab21, and Rab29 mutants by locking them in a GDP-bound state (S17N mutation) and performed a multinucleation assay. This assay is widely used as an indicator of defects in cytokinesis, and we found out that among all the Rabs tested, only Rab14 dominant-negative mutant caused an increase in multinucleated cells (Figure 1B). Importantly, Rab14 KD also led to increased multinucleation (Figure 1C; Supplemental Figure S1A), and Rab14-KD induced a cytokinetic defect that could be rescued by overexpressing shRNA-resistant GFP-Rab14, but not GFP-Rab21 or GFP-Rab25 (Figure 1, C and D).

While a multinucleation assay is a good initial assay to test for cytokinetic defects, it does not provide the information of what stage of cytokinesis is affected. If the defect is in cytokinesis and abscission rather than mitotic spindle formation and chromosome segregation, then dividing cells would be expected to accumulate in telophase. Consistent with Rab14 regulating the abscission, we found that Rab14-KD leads to an increase in telophase cells (Figure 2A). Importantly, the cytokinesis arrest induced by Rab14-KD was similar to the cytokinesis arrest induced by Rab11a/b co-KD (Figure 2A), a known regulator of abscission (Wilson *et al.,* 2005; Simon and Prekeris, 2008; Schiel and Prekeris, 2010; Schiel *et al.,* 2013).

To further understand the role of Rab14 in cytokinesis we next created two HeLa Rab14 KO cell lines (Rab14-KO1 and Rab14-KO2; Supplemental Figure S1, B and C) and performed a time-lapse analysis of cells during mitotic cell division. Consistent with an increase in multinucleation (Figure 2D), about ~17% (8 out of 45) of Rab14-KO cells failed cytokinesis and regressed cleavage furrow to form binucleate cells (Figure 1E; Supplemental Movies S1–S3) while no furrow regressions were observed in control cells (0 out of 75). The remaining 83% of cells did eventually divide but spent a much longer time in anaphase and telophase (Figures 1E and 2C; Supplemental Movie S3). Importantly, similar increases in division time were also observed in Rab14-KD cells (Figure 2B). Abscission defects caused by Rab14-KO could also be rescued by overexpression of GFP-Rab14 (Figure 2C).

Rab14 regulates actin depolymerization at the ICB

Previous studies have demonstrated that Rab11-endosomes are targeted to the ICB and the MB to mediate actin clearance and the establishment of the abscission site (Simon *et al.,* 2008; Schiel *et al.,* 2012). Thus, we next decided to investigate the possible interplay between Rab14 and Rab11 functions during abscission. Our data demonstrate that both Rab11-KD and Rab14-KD lead to delays in division time (Figure 2B), so we next tested the effect of treating HeLa-Rab14-KD cells with Rab11a/b siRNA. As shown in Figure 2B, triple KD of Rab11a, Rab11b, and Rab14 further increased the time required for cell division.

To further investigate the relationship between Rab14 and Rab11, we overexpressed GFP-Rab11a in either Rab14-KD or Rab14-KO cells and analyzed division time, as well as multinucleation. As shown in Figures 1D and 2D, overexpression of GFP-Rab11a was able to rescue cytokinetic defects induced by Rab14 depletion.

Previous studies have shown that Rab11a/b play an important role in cell division by regulating actin clearance from the ICB during cytokinesis (Fielding *et al.,* 2005; Wilson *et al.,* 2005; Dambournet *et al.,* 2011). To find out if Rab14 is also required for actin clearance at the ICB, we costained control or Rab14-KO cells with anti-tubulin antibodies and phalloidin-Alexa 594 (F-actin marker). Consistent with the hypothesis that Rab14 may regulate actin depolymerization during abscission, Rab14 depletion led to an increase in F-actin in the ICB (Figure 2, E and F). Finally, to examine whether the aberrant F-actin accumulation was the cause of the Rab14 depletion-induced cytokinesis defects, we treated control and Rab14-KO cells with a low dose (4 nM) of the F-actin depolymerizing drug Latrunculin A (LatA) and then tested the ability of cells to complete cytokinesis by multinucleation assay. As shown in Figure 2D, LatA treatment rescued Rab14–KO-induced multinucleation while having no effect on multinucleation in control cells.

Rab14 localizes to early endosomes that accumulate at the minus-ends of ICB microtubules during telophase

Our data so far indicate that Rab14 is required for successful completion of cytokinesis, and that just like Rab11, Rab14 appears to function by regulating actin disassembly at the ICB. To further characterize Rab14-dependent cytokinetic steps, we first analyzed Rab14 localization during cell division. To that end, we fixed HeLa cells and costained them with anti-Rab14 and anti-acetylated tubulin (ICB microtubule marker) antibodies. Interestingly, Rab14 was enriched in organelles that during telophase accumulated at the minus-ends of the ICB microtubules (Figure 3, A and B) while similar signal could not be detected in Rab14-KO cells (Figure 3C).

To further characterize Rab14 localization during division, we used CRISPR/Cas9 to create a HeLa cell line with GFP-tagged endogenous Rab14 (Supplemental Figure S2C). We then followed GFP-Rab14 localization at the different stages of mitotic cell division. As shown in Figure 3D, Rab14 is mostly cytosolic (presumably GDP-bound and inactive) during metaphase and anaphase. During telophase, Rab14 accumulates around centrosomes, as well as on endosomelike structures located in close proximity of minus-ends of ICB microtubules (Figure 3D). Interestingly, it has been shown by several studies that Rab11-containing recycling endosomes also accumulate at the minus-end of microtubules, and that this type of accumulation may be required for efficient delivery of recycling endosomes to the ICB and the MB (Simon *et al.,* 2008; Schiel *et al.,* 2012). To determine the identity of these Rab14-containing organelles we next costained telophase and interphase cells with EEA1 (early endosome marker). As shown in Figure 3E, GFP-Rab14 extensively colocalized with EEA1, suggesting that Rab14 is located at the early endosomes, and that these early endosomes are targeted to the close proximity of minus-ends of the ICB microtubules during telophase. Similarly, in interphase cells, Rab14 also colocalized with EEA1, further supporting the findings that Rab14 is a predominately early endosomal protein (Supplemental Figure S2A).

To dissect the possible connection between Rab11- and Rab14-endosomes, we next costained cells with anti-Fip1 antibodies. Fip1 is a well-established Rab11-effector that is present on most Rab11-containing recycling endosomes (Junutula *et al.,* 2004). While Fip1 does not appear to regulate cytokinesis (Wilson *et al.,* 2005), it can be used as a marker for Rab11-containing recycling endosomes during interphase and mitotic cell division (Peden *et al.,* 2004). Little colocalization could be detected between GFP-Rab14 and Fip1 during telophase (Figure 3F), although we could occasionally observe what may be a Fip1-endosome budding from Rab14-containing

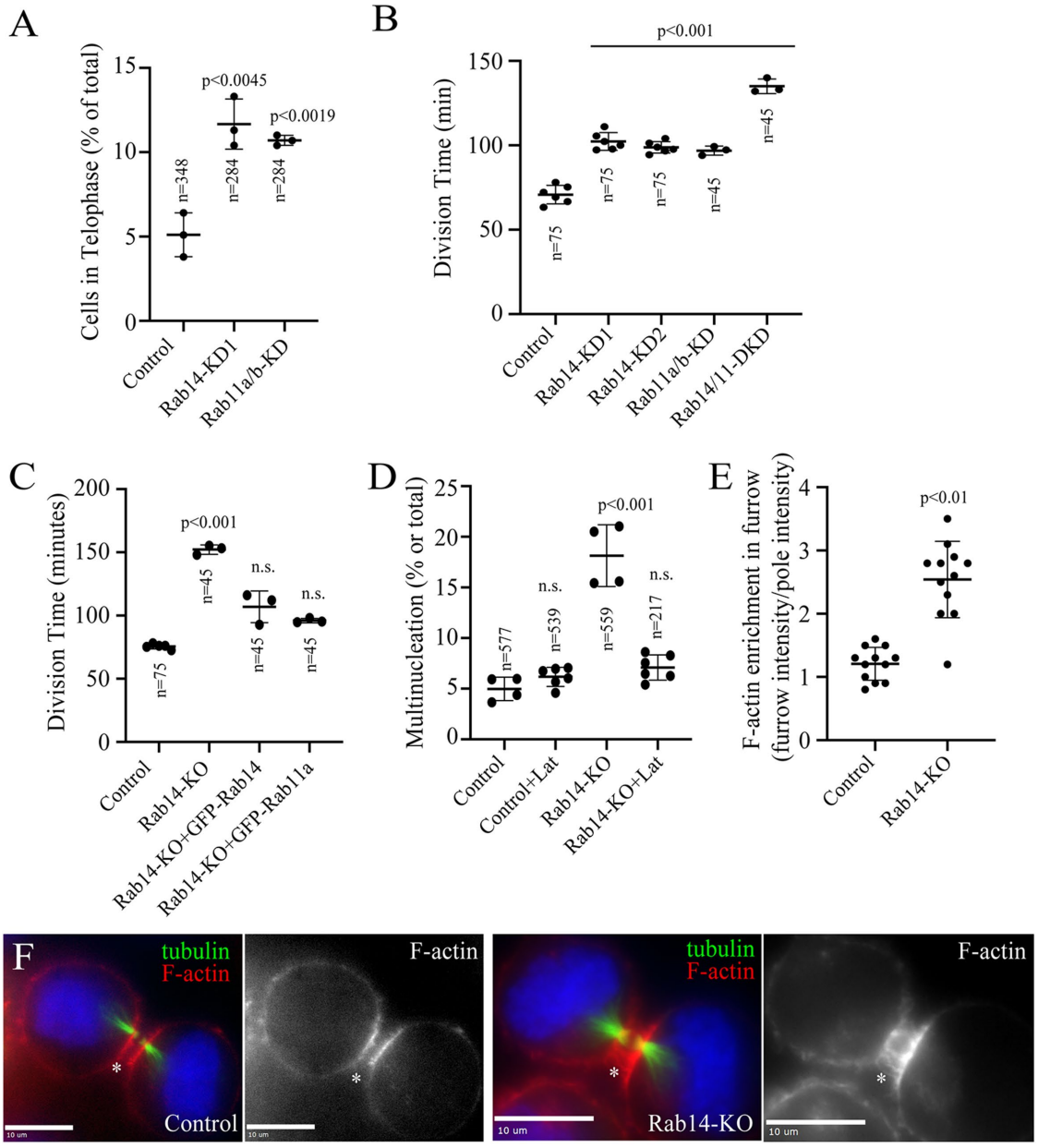

FIGURE 2: Rab14 KD or KO increases time required for cells to complete cytokinesis. (A) Control, Rab14-KD and Rab11a/b-KD cells were fixed and stained with anti-tubulin antibodies to identify cells in telophase. Data shown are the means and SD derived from several independent experiments represented by individual dots; n is the total number of cells counted. (B-C) Control, Rab14-KD, Rab11a/b-KD, Rab14/11-DKD, and Rab14-KO cells were analyzed by time-lapse microscopy to measure the time needed to complete division (starting from metaphase). Where indicated, cells were transiently transfected with GFP-Rab11a or GFP-Rab14. Data shown are the means and SD derived from several independent experiments represented by individual dots; *n* is the total number of cells counted. (D) Control or Rab14-KO cells were incubated in the absence or presence of 4 nM LatA and multinucleated cells counted to assess their ability to complete cytokinesis. Data shown are the means and SD derived from several independent experiments represented by individual dots; *n* is the total number of cells counted. (E, F) Control or Rab14-KO HeLa cells were fixed and stained with phalloidin-594 and anti-tubulin antibodies. The enrichment of phalloidin-594 at the ICB was then evaluated. Scale bars represent 10 μm. The quantification is shown in F. The data are expressed as the ratio between phalloidin-594 fluorescence intensity at the ICB (intensity per area) and opposing cell poles (intensity per area). Data shown are the means and SD derived from three independent experiments. Dots represent the number of cells analyzed.

early endosome (Figure 3E, see inset). Thus, we speculate that Rab14 and Rab11 could be part of the same endocytic pathways, with Rab11-containing endocytic carriers budding from Rab14-containing early endosomes, although further analysis will be needed to determine that.

Rab14 is regulates the targeting of Rab11/Fip3-endosomes during cytokinesis

Our localization data suggest that Rab11-recycling endosomes may bud directly from Rab14-containing early endosomes that are situated at the minus-ends of ICB microtubules during telophase. This

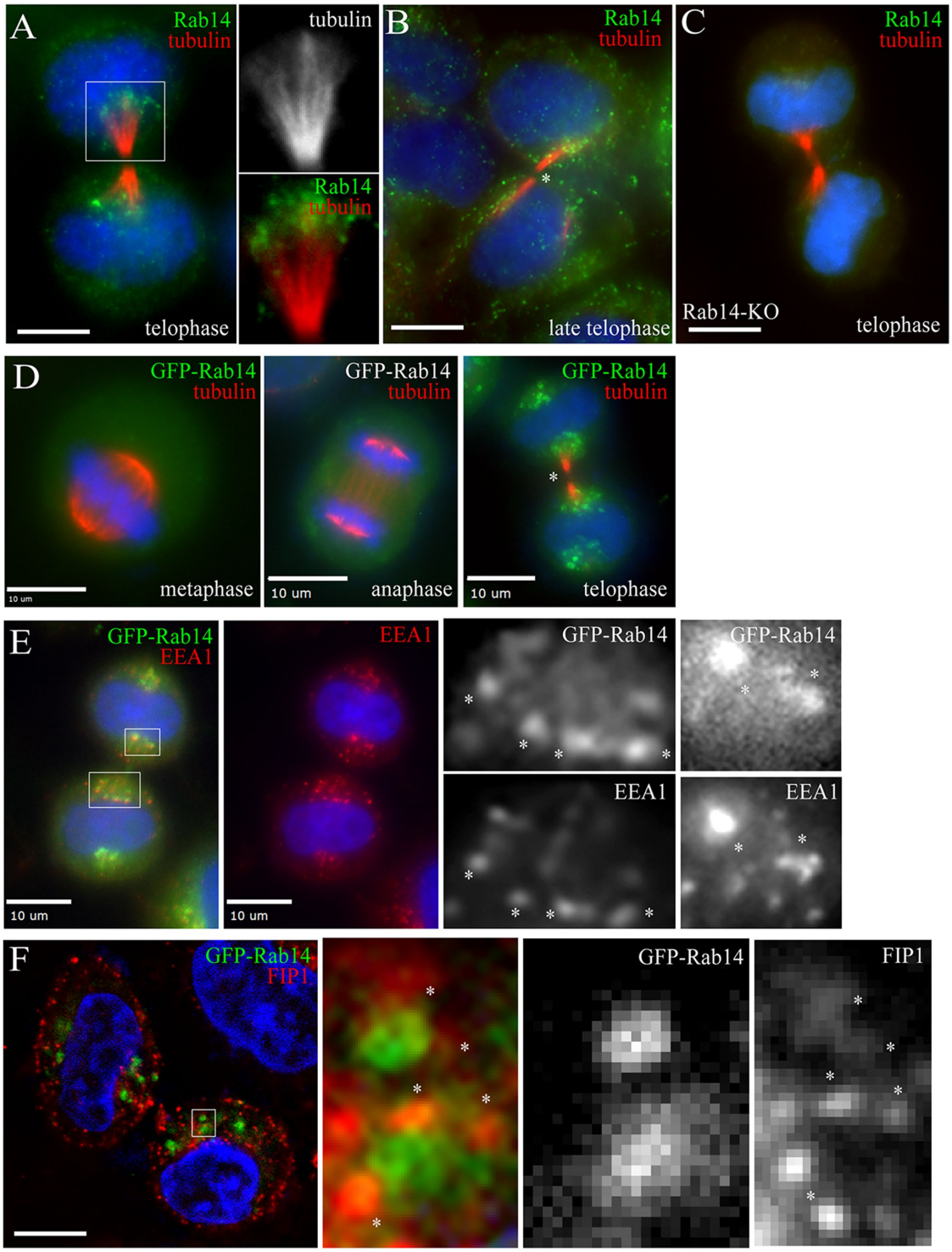

FIGURE 3: Rab14 is enriched at early endosomes located at the minus-ends of the ICB microtubules. (A–C) HeLa cells in telophase were fixed and stained with anti-Rab14 and anti-tubulin antibodies. A and B show control HeLa cells, while C shows Rab14-KO HeLa cells. Scale bars represent 10 μm. The asterisk marks the ICB and the box in A marks the region represented in higher magnification insets. (D–F) HeLa cells expressing GFP-tagged endogenous Rab14 were fixed and stained with anti-tubulin (D), anti-EEA1 (E), or anti-Fip1 (F) antibodies. Asterisks mark the ICB (A–D), EEA1 and Rab14-positive endosomes (E), or Rab14-positive endosomes associated with Fip1-endosomes (F). Scale bars represent 10 μm.

raises an interesting possibility that positioning of Rab14-endosomes at the minus-ends of the ICB microtubules may regulate the targeting of newly formed Rab11-recycling endosomes to the ICB and the MB. To test this hypothesis, we investigated the localization of Rab11/Fip1-endosomes during telophase in the control and Rab14-KO cells. Since some reports suggested that Rab14 can directly bind to Fip1 (Kelly *et al.*, 2009; Lall *et al.*, 2015), we first tested whether Rab14-KO affects Fip1 recruitment to endosomes. As

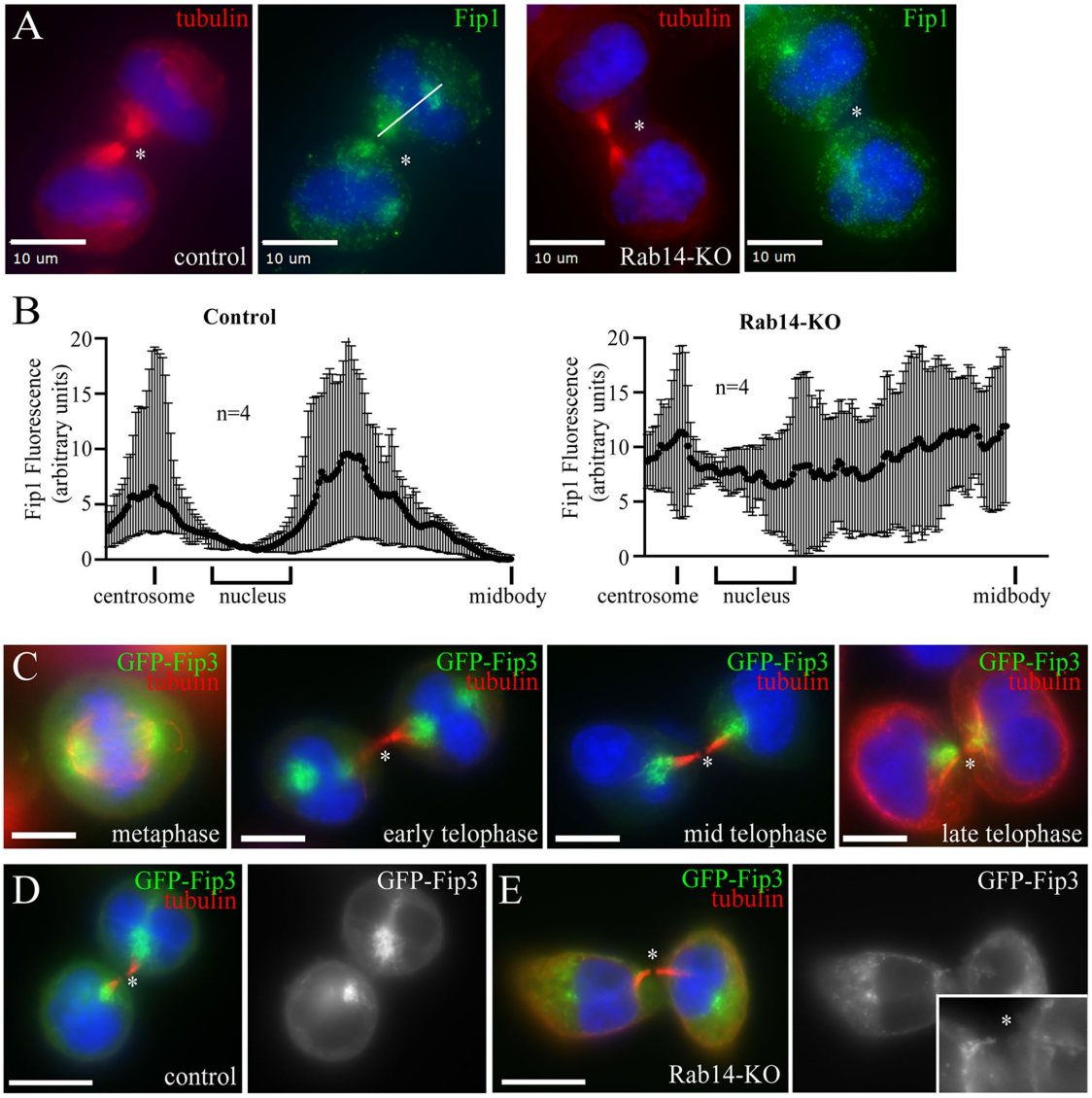

FIGURE 4: Rab14 is required for targeting Fip1- and Fip3-endosomes to the ICB microtubules. (A, B) Control or Rab14-KO HeLa cells were fixed and stained with anti-tubulin and anti-Fip1 antibodies. Line-scan analysis of Fip1 fluorescence was then performed in telophase cells (see line in A). Asterisks mark the ICB. Data shown in B are the means and SD derived from line-scans of four different cells. Scale bars represent 10 μm. (C, D) Control or Rab14-KO HeLa cells expressing GFP-Fip3 were fixed and stained with anti-tubulin antibody. Scale bars represent 10 μm.

shown in Supplemental Figure S2B, Fip1 targeting to endosomes in interphase cells was not affected by Rab14-KO. Next, we analyzed the distribution of Fip1 during telophase. As shown in Figure 4, A and B, in agreement with previously published reports, Rab11-recycling endosomes (as determined by Fip1 localization) accumulate at the ICB microtubules during telophase and this accumulation is diminished by Rab14-KO.

To further investigate the effect of Rab14 KO on recycling endosome targeting to the ICB, we transfected cells with GFP-Fip3 and analyzed recycling endosome dynamics by time-lapse microscopy. Fip3 is also a Rab11-interacting protein that has been directly implicated in regulating abscission by delivering p50RhoGAP and contributing to actin depolymerization at the abscission site (Schiel *et al.*, 2012). Unlike Fip1 that localizes to most Rab11-recycling endosomes, Fip3 only localizes to a subset of recycling endosomes that are targeted to the MB and the abscission site (Simon *et al.*, 2008; Prekeris 2015), making Fip3 an excellent marker to monitor the dynamics of these endosomes during cytokinesis. As shown in Figure 4C (also see Supplemental Movies S4–S5 and Supplemental Figure S2D), in control HeLa cells, GFP-Fip3-endosomes move from centrosomes to the ICB as cell completes division (in 81.5% of cells; 27 dividing cells analyzed). In contrast, in Rab14-KO cells, GFP-Fip3-endosomes accumulate at the centrosome, but then fail to relocalize to the ICB at late telophase (in 90% of cells; 20 dividing cells analyzed) (Figure 4, D and E; Supplemental Movies S6 and S7). Taken together, our data suggest that Rab14 may contribute to targeting of early endosomes to the minus-ends of the ICB microtubules and consequently affecting the delivery of Rab11/Fip3-endosomes to the abscission site.

MACF2 is a Rab14-binding protein that regulates cytokinesis

While our data suggest that Rab14 is required for endosome targeting to minus-ends of the ICB microtubules, the molecular machinery

governing Rab14 function during telophase remains unclear. Keeping in mind that all Rab proteins function via GTP-dependent interactions with a diverse array of specific effector proteins (Hutagalung and Novick, 2011), we decided to identify Rab14 effector proteins that function in cell division. To that end, we next created HeLa cells stably expressing either FLAG-Rab14 or FLAG-Rab14-Q70L (constitutively active Rab14 mutant) and performed coimmunoprecipitation/proteomics analysis from synchronized HeLa cells in telophase using anti-FLAG antibody. Since Rab GTPases bind to their effectors in a GTP-dependent manner, we filtered all candidate proteins based on two main criteria: 1) the candidate proteins should not be present at IgG control and 2) the candidate proteins should be enriched at least 2× in the Rab14-Q70L sample (Figure 5A). Proteomic analysis identified nine candidates that appear to be interacting specifically with GTP-bound Rab14 (Figure 5A). One of these proteins, MACF2 (microtubule actin cross-linking factor 2), is a large scaffolding protein that belongs to a spectraplakin family and is implicated in microtubule bundling, cross-talk between actin and microtubules, as well as regulating noncentrosomal microtubule dynamics (Sun *et al.,* 2001; Noordstra *et al.,* 2016). Furthermore, MACF1, also known as ACF7, is a closely related MACF2 isoform that was shown to bind to CAMSAP3/Patronin proteins and interact with microtubule minus-ends (Noordstra *et al.,* 2016). Finally, MACF1 was shown to be required for Rab11-endosome traffic during epithelia polarization (Noordstra *et al.,* 2016), so this raises an interesting possibility that MACF2 may also interact with CAMSAP3 and regulate Rab11-endosome targeting during cytokinesis. Testing this hypothesis is the focus of the rest of this study.

To confirm that MACF2 is a Rab14-interacting protein, we used a GST-tagged anti-GFP nanobody to pull down the endogenously tagged GFP-Rab14 using a glutathione bead pull-down assay, followed by immune-blotting using anti-MACF2 antibodies. As shown in Figure 5B, MACF2 was pulled down only when Rab14 was loaded with a nonhydrolysable GTP analogue, GTPγS, an observation consistent with MACF2 being a Rab14 effector protein. Since MACF1 was shown to interact with CAMSAP3, a microtubule minus-end interacting protein, we wondered whether MACF2 and Rab14 complex also interacts with CAMSAP3. Consistent with this hypothesis, anti-GFP-nanobodies coimmunoprecipitated CAMSAP3 with GFP-Rab14. Importantly, CAMSAP3 also coprecipitated predominately with GTP-locked GFP-Rab14 (Figure 5B), suggesting that MACF2 and CAMSAP3 interact with activated Rab14.

To further confirm that Rab14 interact with MACF2, we incubated cellular lysates with glutathione beads coated with either GST-only or purified GST-Rab14. As shown in the Figure 5B, GST-Rab14 beads could pull down MACF2 in a GTP-dependent manner, thus further confirming that MACF2 may be Rab14 effector protein.

To determine whether MACF2/CAMSAP3 are important for cytokinesis, we next transfected cells with Halo-MACF2 or GFP-CAMSAP3 and analyzed its localization during telophase in HeLa cells. Unfortunately, despite our efforts, we were unable to get HeLa cells to express Halo-MACF2 at the levels that could be used for imaging. Thus, we decided to focus on CAMSAP3. Interestingly, GFP-CAMSAP3 was highly enriched at the ICB microtubules (Figure 5C), consistent with its role in regulating/protecting minus-ends of noncentrosomal microtubule bundles (Noordstra *et al.,* 2016). Importantly, Rab14-KO did not have any effect on GFP-CAMSAP3 localization (Figure 5, D and F) suggesting that both, CAMSAP3 and possibly MACF2, are targeting to the ICB independent of Rab14 (presumably by direct binding to microtubules). Thus, we suggest that MACF2 and CAMSAP3 together play a role in modulating abscission.

To better understand MACF2 functions during cell division, we used two different shRNAs (MACF2-KD1 and MACF2-KD2) to deplete MACF2 in HeLa cells (Supplemental Figure S3A). Interestingly, MACF2 depletion decreased localization of GFP-CAMSAP3 to the ICB microtubules (Figure 5, E and F), suggesting that MACF2 may regulate this process. We performed time-lapse analysis to test the effect of MACF2 depletion on time required for cells to complete abscission, and as shown in Figure 6, A and B (also see Supplemental Movie S8), MACF2 depletion increased overall cell division time from 70 min in control cells to 132 min in HeLa-MACF2-KD1 and to 124 min in HeLa-MACF2-KD2 cells. Overall, these results suggest that MACF2 is a Rab14 effector protein and is another important regulator of cell division.

MACF2 is required for Fip3-endosome targeting to the ICB

Since Rab14 depletion does not affect MACF2 or CAMSAP3 targeting to the ICB, we hypothesized that MACF2 may function as a tether anchoring Rab14-containing early endosomes at the ICB microtubules during early telophase. To test this hypothesis, we stained the control or MACF2-KD cells with anti-Fip1 antibody to analyze the localization of Rab11-endosomes during telophase. Consistent with the involvement of MACF2 in regulating endocytic transport to the ICB, MACF2 depletion inhibited accumulation of Rab11/Fip1-endosomes at the minus-ends of the ICB microtubules (Figure 6, C and D). Similarly, MACF2 KD also inhibited Rab14 accumulation at the minus-ends of ICB microtubules (Figure 6, E and F).

We next wondered whether the depletion of MACF2 would also affect trafficking of Rab11/Fip3-endosomes to the abscission sites at the ICB. For this purpose, we transfected control and MACF2-KD1 cells with GFP-FIP3 construct and performed time-lapse imaging analysis. As shown in Supplemental Figure S3D, FIP3 localization at the ICB during late telophase was disrupted by the depletion of MACF2 (in 85.2% of cells; 27 dividing cells analyzed) (also see Supplemental Movie S9; for control, refer to Supplemental Figure S2D). Altogether, these results suggest that MACF2 and CAMSAP3 complex may regulate Rab14- and Rab11-endosome targeting to the ICB microtubules during early telophase, thus mediating the actin clearance during mitotic cell division.

DISCUSSION

Abscission is the last step of mitotic cell division that leads to resolution of the ICB and physical separation of two daughter cells. It is now becoming clear that abscission is a very complex and highly regulated event (Schiel and Prekeris, 2010; Addi *et al.,* 2018; Fremont and Echard, 2018). Indeed, recent studies identified a new mitotic checkpoint, known as abscission checkpoint, that is activated by lagging chromosomes and leads to the arrest of the cells in telophase (Sadler *et al.,* 2018; Bai *et al.,* 2020; Petsalaki and Zachos, 2020). We now know that abscission involves highly organized remodeling of the cytoskeleton at the ICB. Specifically, the abscission site is defined by severing of ICB microtubules and localized disassembly of actin cytoskeleton that is presumably a remnant of the cytokinetic contractile ring (Schiel *et al.,* 2012; Schiel and Prekeris, 2013; Fremont *et al.,* 2017b; Addi *et al.,* 2018; Fremont and Echard, 2018). Here we define a new Rab14 and MACF2-dependent pathway that is needed for F-actin clearance from the ICB and for successful completion of cytokinesis.

Recycling endosomes have emerged as key regulators of localized actin disassembly and completion of abscission. It was shown that various regulators of actin depolymerization, such as MICAL1, p50RhoGAP, and OCRL, are all delivered by two distinct sets of

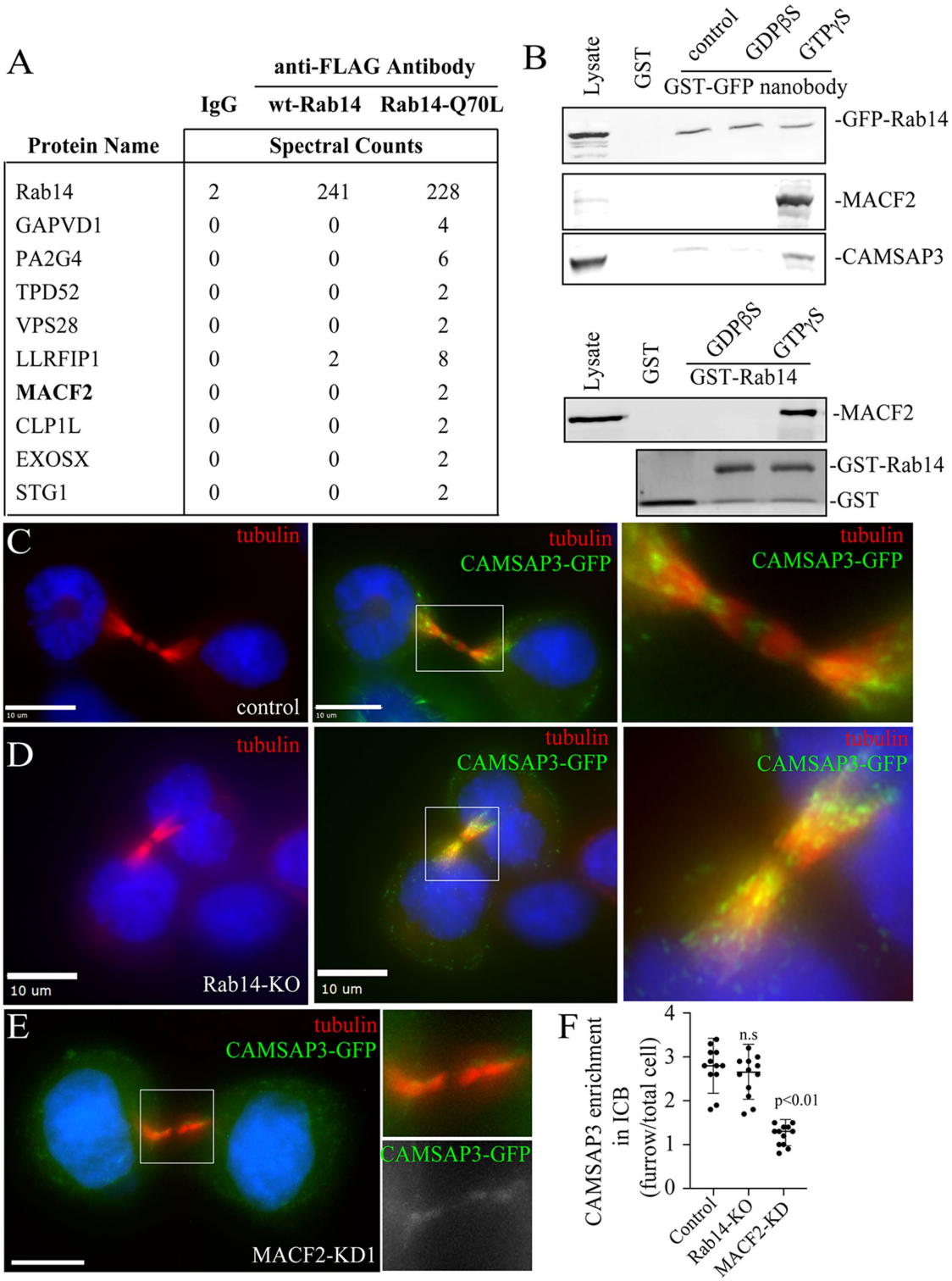

FIGURE 5: Rab14 binds to MACF2/CAMSAP3 complex. (A) Putative Rab14-interacting proteins identified in FLAG-Rab14 immunoprecipitation and proteomic analysis. (B) In the top panels, lysates from HeLa cells expressing endogenously labeled GFP-Rab14 were incubated with either glutathione beads coated with GST or GST-anti-GFP-nanobody. The beads were then washed and bound protein was analyzed by Western blotting. In the bottom panels, HeLa cell lysates were incubated with glutathione beads coated with either GST-only or GST-Rab14. Beads were then washed, and bound proteins were eluted and either blotted with anti-MACF2 or stained with Coomassie stain. (C–F) Control (C), Rab14-KO (D), or MCF2-KD (E) HeLa cells were transiently transfected with GFP-CAMSAP3 and then fixed and stained with anti-tubulin antibody. (F) Quantification of GFP-CAMSAP3 enrichment at the ICB. The data are expressed as the ratio between GFP-CAMSAP fluorescence intensity at the ICB (intensity per area) and total cellular GFP-CAMSAP3 fluorescence intensity (intensity per area). Data shown are the means and SD derived from three independent experiments. Dots represent the number of analyzed cells. Scale bars represent 10 μm.

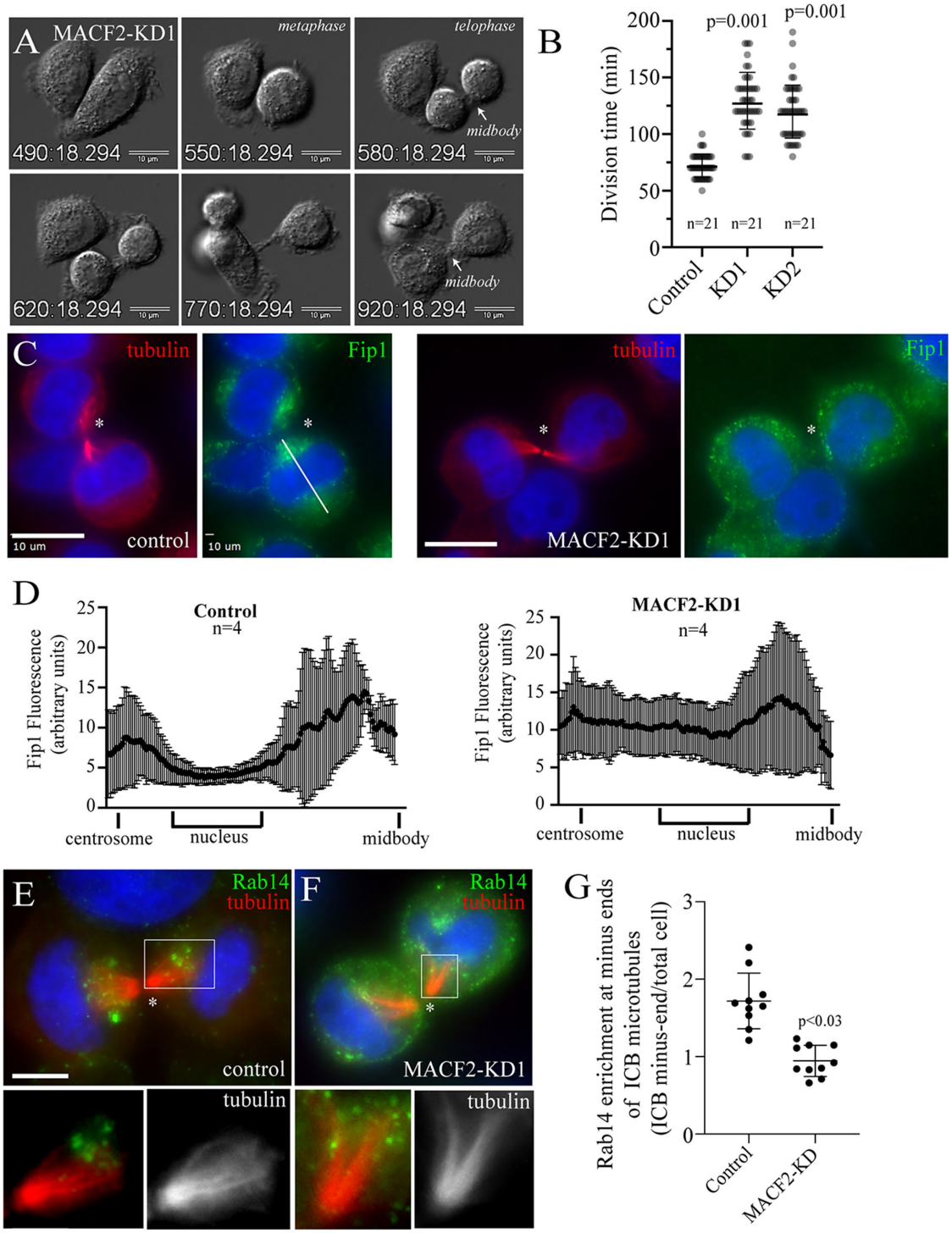

FIGURE 6: MACF2 is required for completion of cytokinesis and for targeting of Rab11-endosomes to the ICB microtubules. (A, B) Time-lapse images of dividing MACF2-KD1 HeLa cell. Time units listed on the images are minutes. (B) Quantification of time required for completing division (starting from metaphase). Data shown in B are the means and SD derived from three independent experiments. Dots represent the number of cells analyzed by time-lapse microscopy. (C, D) Control or MACF2-KD1 cells were fixed and stained with anti-tubulin and anti-Fip1 antibodies. Line-scan analysis of Fip1 fluorescence was then performed in telophase cells (see line in C). Asterisks mark the ICB. Data shown in D are the means and SD derived from line-scans of four different cells. Scale bars represent 10 μm. (E, G) Control or MACF2-KD1 cells were fixed and stained with anti-tubulin and anti-Rab14 antibodies. Asterisks mark the ICB. (D) Quantification of the Rab14 enrichment at the minus-ends of ICB microtubules. The data are expressed as the ratio between Rab14 fluorescence intensity at the ICB (intensity per area) and total cellular Rab14 fluorescence intensity (intensity per area). Data shown are the means and SD derived from three different experiments. Each dot represents individual cell analyzed. Scale bars represent 10 μm.

recycling endosomes, Rab11- and Rab35-endosomes (Dambournet *et al.,* 2011; Collins *et al.,* 2012; Schiel *et al.,* 2012; Fremont *et al.,* 2017b). It is now believed that rapid and highly targeted delivery of these actin regulators to the abscission site is dependent on ICB microtubules to transport Rab11- and Rab35-endosomes, rather than relying on passive diffusion from cytosol to the microtubule-packed ICB. ICB microtubules are perfectly suited for this task since they are arranged in a polarized manner with plus-ends oriented toward the center of the ICB where they form a unique structure known as the MB. What remains to be fully understood is how these endosomes are targeted to the ICB microtubules where they can engage with molecular motors to be delivered to the forming abscission site. Interestingly, numerous studies have shown that during metaphase and anaphase, Rab11-endosomes accumulate around the centrosome, although the machinery mediating centrosomal accumulation remains unclear (Collins *et al.,* 2012; Schiel *et al.,* 2012). Once a cell enters telophase, Rab11-endosomes leave the centrosome and transiently accumulate around minus-ends of the ICB microtubules before entering the ICB and mediating cell abscission (Simon *et al.,* 2008; Hoog *et al.,* 2011). The function of this endosome accumulation at the minus-ends of ICB microtubules remains unclear, but it could be hypothesized that this accumulation helps with loading of Rab11-endosomes for plus-end-directed (kinesin-dependent) transport to the abscission site. In this study we identify Rab14 as a protein that may be involved in regulating endosome accumulation at the ICB microtubules and also demonstrate that depletion of Rab14 leads to delay or failure of the abscission.

We originally identified Rab14 as one of several endocytic Rabs present in the MB proteome (Figure 1A) (Peterman *et al.,* 2019). Importantly, our analysis shows that, in addition to Rab11 and Rab35 (also identified in MB proteome), Rab14 is also a MB-associated Rab that is required for cytokinesis, since depletion of Rab14 or expression of Rab14 dominant-negative mutant leads to a significant increase in time required for abscission or complete abscission failure. These data led us to hypothesize that Rab14 may mark the endosomes that deliver yet another actin regulator to the abscission site. Surprisingly, our time-lapse and immunofluorescence analyses show that Rab14-endosomes accumulate at the minus-ends of the microtubules. Additionally, Rab14 appears to be predominantly present on early endosomes that also contain EEA1 and presumably Rab5. Since it has been shown that Rab11-containing recycling endosomes bud from early endosomes, we hypothesized that Rab14 may mediate targeting of early endosomes to the minus-ends of the ICB microtubules, thus ensuring efficient formation and targeting of Rab11/Fip3-endosomes to the ICB microtubules and the abscission site. Consistent with this hypothesis, Rab14 depletion decreased Fip3-endosome accumulation at the ICB microtubules, as well as inhibited actin disassembly at the ICB during abscission. Furthermore, Rab14-KO-dependent abscission phenotypes can be rescued by overexpressing of Rab11, indicating that Rab11 may function downstream of Rab14. An alternative possibility is that Rab14- and Rab11-endosomes are part of two separate and parallel pathways that are both involved in regulating actin depolymerization at the ICB. Indeed, regulation of actin dynamics during abscission was shown to be mediated by both Rab35 and Rab11, both marking a distinct subset of endosomes (Dambournet *et al.,* 2011; Schiel *et al.,* 2013). Thus, Rab14 may be just another redundant pathway in this process. That would be consistent with published observations, as well as data in this study, that KO or KD of Rab11, Rab14, and Rab35 individually only partially blocks cell ability to complete abscission. Further work will be needed to fully understand the relationship among Rab35, Rab11, and Rab14.

To determine how Rab14 itself is targeted to minus-ends of ICB microtubules, we next completed Rab14 immunoprecipitation/proteomic analysis using HeLa cells synchronized in telophase. Importantly, proteomic analysis followed by pull-down assays identified MACF2 as a Rab14-interacting protein. What makes MACF2 such an interesting protein is that it is known to bind both actin and microtubules, as well as mediate microtubule bundling. Additionally, MACF1, a closely related MACF2 paralogue, was shown to bind to CAMSAP3 and mediate targeting of MACF1/CAMSAP3 to minus-ends of microtubules in epithelial cells (Noordstra *et al.,* 2016). Since CAMSAP3 can coimmunoprecipitate with Rab14 and MACF2, we propose that MACF2/CAMSAP3 complex tethers Rab14 to the minus-ends of the ICB microtubules, mediating targeting of early endosomes and consequently Rab11-endosomes to the MB and abscission site. Consistent with this hypothesis, we show that CAMSAP3 localizes to the ICB microtubules during abscission. Importantly, MACF2 depletion also inhibits CAMSAP3 targeting to the ICB microtubules, as well as accumulation of Rab11- and Rab14-endosomes at the ICB microtubules.

Based on all our data we propose that Rab14 and MACF2 play an important role in targeting endosomes to the ICB microtubules. However, many questions remain and further studies will be needed to answer them. Does Rab14 also regulate targeting of Rab35-endosomes? What drives formation of the Rab14/MACF2/CAMSAP3 complex during telophase, but blocks it from functioning in metaphase and anaphase? Interestingly, Rab14 was also implicated in regulating epithelial cell polarity (Lu and Wilson, 2016), as well as recycling of integrins during cell migration (Gundry *et al.,* 2017). Both of these cellular processes are also dependent on actin and microtubule dynamics, thus it will be interesting to see whether Rab14 interaction with MACF2/CAMSAP3 complex may have functions during cell polarization and migration.

MATERIALS AND METHODS

Request a protocol through *Bio-protocol.*

Cell culture and treatments

Cells were grown in 37°C humidified incubator at 5% CO_2, routinely tested for mycoplasma, and were maintained in DMEM with 10% fetal bovine serum and 1% penicillin/streptomycin. To create FLAG-Rab14 stable cell line, HeLa cells were infected with lentivirus pLVX:FLAG-Rab14. To create FLAG-Rab14-Q70L stable cell line, HeLa cells were infected with lentivirus pLVX:FLAG-Rab14-Q70L.

Stable Rab14 KO HeLa cell line (HeLa-Rab14-KO) was generated by using Dharmacon human Rab14 crRNAs (51552).

Rab11 RNA interference in HeLa and HeLa-Rab14-KD2 cells was performed by using QIAGEN HP Custom siRNAs (Rab11a and Rab11b).

Stable Rab14 KD HeLa cell lines (HeLa-Rab14-KD1 and HeLa-Rab14-KD2) were generated by using Sigma lentiviral human Rab14 shRNA plasmids (TRCN0000293339 and TRCN000293336). Stable ACF7 KD HeLa cell lines (HeLa-MACF2-KD1 and HeLa-MACF2-KD2) were generated by using Sigma lentiviral human MACF2 shRNA plasmids (TRCN0000300045 and TRCN0000303930). Lentivirus expressing scrambled shRNA was used as negative control. HeLa cell populations expressing either Rab14 or MACF2 shRNAs were selected with puromycin, expended and frozen as stocks, and then used in all experiments. To diminish the accumulation of aneuploidy or polyploidy, we only used cells up to passage 10.

Antibodies

The following antibodies were used for immunofluorescence and Western blots: acetylated-α-tubulin (Cell Signaling, D20G3, IF 1:200, WB 1:1000), Rab14 (Sigma-Aldrich, R0656, IF 1:100, WB 1:500), FLAG (Sigma-Aldrich, F1804, IF 1:100, WB 1:1000), and MKLP1 (Thermo Fisher, PA5-31773, IF 1:200). The Alexa 594– and Alexa 647–conjugated anti-mouse and anti-rabbit secondary antibodies used for immunofluorescence were purchased from Life Technologies. The IRDye 680RD Donkey anti-mouse and IRDye 800CW donkey anti-rabbit secondary antibodies used for Western blotting were purchased from LI-COR Biosciences (Lincoln, NE). Phalloidin conjugated to Alexa Fluor 594 (A12381) was purchased from Thermo Fisher Scientific (Eugene, OR), and LifeAct-mCherry (54491) was bought from Addgene (Michael Davidson). During coimmunoprecipitation, FLAG antibody (Sigma-Aldrich, F3165) was cross-linked to Protein G–Sepharose beads. HaloTag Alexa Fluor 488 Ligand (G1002) was purchased from Promega (Madison, WI).

RNA isolation and quantitative PCR (qPCR)

RNA was isolated by using PureLink RNA Mini Kit as per the manufacturer's instructions (Invitrogen, Carlsbad, CA). cDNA was obtained by using the High Capacity RNA to cDNA Kit as per the manufacturer's instructions (Applied Biosystems, Foster City, CA). qPCR was performed by using TaqMan probes (Applied Biosystems, Pleasanton, CA). TaqMan probes used were: Hs03929097 (*GAPDH*) and Hs00156137 (*MACF2*). For quantification, Ct values were normalized to GAPDH and then normalized to control cells.

Multinucleation assay

Control or various KD or KO cells, or cells overexpressing GFP-tagged dominant-negative mutants, were seeded on collagen I-coated (at final 50 μg/ml concentration, Thermo Fisher Scientific, Grand Island, NY) glass coverslips. After 48 h in the culture, the cells were fixed in 4% paraformaldehyde, permeabilized with 0.2% Triton X-100 for 3 min at room temperature, and stained with Alexa Flour 594 phalloidin (Thermo Fisher Scientific, Eugene, OR) for 30 min at 37°C. The coverslips with cells were mounted on 3-cm glass-bottom cell culture plates using Vectashield mounting medium with DAPI (Vector Laboratories, Burlingame, CA). Random fields on the coverslips were photographed using an inverted Olympus IX81 microscope (Olympus Europe Holding Gmbh, Germany, Hamburg) with a 20× oil immersion lens, and the number of multinucleated cells was counted manually. The rate of total multinucleated cells was then calculated in five randomly chosen fields. To analyze the effect of GFP-tagged dominant-negative Rab mutants, only cells expressing low-to-moderate levels of GFP were analyzed. All data are derived from at least three independent experiments.

To rescue multinucleation, either HeLa-Rab14-KD2 or HeLa-Rab14-KO cells were seeded on collagen-coated glass coverslips and transiently transfected with various GFP-tagged Rab plasmids. Then 48 h posttransfection, cells were processed and examined for multinucleation as described above. Only cells expressing GFP-tagged Rab were analyzed and only low-to-moderate levels of GFP-tagged proteins (as estimated by immunofluorescence microscopy) were used for this analysis.

To examine LatA effect on rescuing multinucleation, HeLa-Rab14-KO cells were seeded on collagen-coated glass coverslips and treated with 4 nM concentration of LatA overnight. After 24 h cells were processed and examined for multinucleation as described above.

Immunofluorescence and time-lapse microscopy

All fixed cells were imaged with an inverted Olympus IX81 microscope (Olympus Europe Holding Gmbh, Hamburg, Germany) using PlanApo N 60×/1.42 oil lens and the Orca-R^2 digital camera with excitation system MT10. Image processing was carried out by using the XCELLENCE software.

Time-lapse analysis. To measure overall cell division time and the time that cells spend in each mitotic stage, 40,000 cells were plated on fibronectin-coated (at final 30 μg/ml, Sigma Aldrich, CO) 3-cm glass-bottom cell culture plates. After 48 h in culture, the plates were placed in a heat- and humidity- (37°C, 5% CO_2) controlled incubator (INUBG2EONICS Tokai Hit, Shizuoka-ken, Japan) mounted on top of the motorized XY stage. Cells were imaged using an inverted Olympus IX81 microscope (Olympus Europe Holding Gmbh, Hamburg, Germany) with a 20× oil immersion objective, and images were acquired every 10 min. During time-lapse analysis we identified different mitotic stages using following criteria: 1) cells start metaphase when they round up and chromosomes are aligned in metaphase plate (as determined by DIC); 2) cells enter anaphase when cells start elongating due to movement of opposing poles; 3) telophase starts when cells initiate cytokinetic furrow; 4) cells complete cytokinesis when we cannot observe clearly identifiable MB and the ICB. In all cases, the data are derived from at least three independent experiments.

To rescue overall cell division time and the time that cells require to complete each stage of the mitotic phase, either 40,000 control or HeLa-Rab14-KO cells were plated on fibronectin-coated 3-cm glass-bottom cell culture plates and transiently transfected with GFP-Rab14 or GFP-Rab11a plasmids. Then 24 h posttransfection, the cells were analyzed by time-lapse imaging as described above. Only cells expressing low-to-moderate levels of GFP-Rab14 or GFP-Rab11a (as determined by microscopy) were used for this analysis.

To determine the effect of Rab11 siRNA on overall cell division time, either control or HeLa-Rab14-KD2 cells were transfected with Rab11a/b siRNAs. Then 24 h posttransfection cells were plated on fibronectin from bovine plasma (at final 30 μg/ml, Sigma Aldrich, CO) coated 3-cm glass-bottom cell culture plates. After 48 h in culture, the cells were analyzed by time-lapse imaging as described previously.

To study Fip3 localization during cell division using time-lapse microscopy, cells were plated on fibronectin-coated glass-bottom cell culture plates. After 24 h in culture, the cells were transiently transfected with GFP-Fip3 plasmid. Then 24 h posttransfection, the cells were analyzed by time-lapse imaging as described above. Only cells expressing low-to-moderate levels of GFP-Fip3 were used for analysis.

Mitotics tage analysis. To determine the fraction of cells in metaphase and telophase control or Rab14-KD cells were fixed and stained with DAPI and anti-tubulin antibodies. Cells in metaphase or telophase were identified based on mitotic spindle and chromatin condensation status. Cells were counted in 30 randomly selected fields in each of independent experiments and expressed as a percentage of all cells present in the field.

Line-s can analysis. To perform a line-scan analysis of Fip1 distribution, four cells (for each experimental condition) in midtelophase were picked. The midtelophase was defined by three major criteria: 1) cells were still round up; 2) the ICB was still short and not extended; 3) nucleus was "bean shape" rather than circular. A line was drawn through the ICB and presumptive centrosomal pool of

Fip1-endosomes (present on the outer periphery of the nucleus). The values from individual cells were then averaged and shown as means and SD.

F-actin, CAMSAP3, and Rab14 enrichment in the ICB analysis. To measure F-actin, Rab14, or CAMSAP3 fluorescence at the ICB, we generate a z-stack of the cell in telophase using 200-nm Z-step size. The single-image plane from the Z-stack then was selected based on where it includes the entire ICB in focus. The regions of interest (ROIs) were then selected at the ICB (for F-actin or CAMSAP3) or at the minus-ends of ICB microtubules (for Rab14). For control, ROIs were selected either at opposing poles of the cell (for F-actin analysis) or the entire daughter cells (for CAMSAP3 and Rab14 analyses). Fluorescence was then measured (as sum-fluorescence) and normalized to the size of ROI. Finally, the ratios of fluorescence in the ICB and poles (F-actin), ICB and entire cell (CAMSAP3), or minus-ends of ICB microtubules and entire cell (Rab14) were calculated to measure the enrichment of the F-actin, CAMSAP3, or Rab14 at the ICB.

Immunoprecipitation and proteomic analysis

Coimmunoprecipitation was performed using HeLa-FLAG-Rab14 and HeLa-FLAG-Rab14-Q70L cell lines. Cells were synchronized using thymidine/nocodazole block as described previously (Schiel *et al.*, 2012). Cells were collected at telophase and Triton X-100 lysates were used for immunoprecipitation using anti-FLAG antibody conjugated to Protein G–Sepharose beads and analyzed by mass spectrometry as described previously (Schiel *et al.*, 2012). All proteins identified by mass spectrometry were filtered using following criteria: 1) not present in IgG control sample and 2) enriched at least 2× in Rab14-Q70L sample. Additionally, we eliminated all RNA- and DNA-binding proteins, as well as all mitochondria proteins as putative contaminants. The final list is shown in Figure 5A.

CRISPR/Cas9-mediated GFP tagging of endogenous Rab14

A HeLa cell line with GFP-tagged endogenous Rab14 was generated via coelectroporation of CRISPR/Cas9 ribonucleoproteins (RNPs) and linear double-stranded DNA homology-directed repair template (HDRT) (see Supplemental Figure 2A), based on the method of Roth *et al.* (2018). A guide RNA (gRNA) sequence of GTATGGTGCAGTTGCCATGG, which targets in the start codon of Rab14, was selected using the CRISPR gRNA design tool (Haeussler *et al.*, 2016) to identify the gRNA with the highest specificity and efficiency within ~30 nt of the 5′ end of Rab14 exon 1. To generate this gRNA, the crRNA and tracrRNA components were synthesized by Thermo Fisher Scientific (Waltham, MA) and were annealed according to the manufacturer's protocol. The HDRT consisted of a superfolder GFP (Pedelacq et al., 2006) coding sequence flanked by 350–400 bp homology arms for the genomic regions upstream (the 5′UTR of Rab14) and downstream (Rab14 exon 1 in-frame with GFP and a portion of intron sequence). This HDRT was synthesized by Integrated DNA Technologies (Coralville, IA), amplified by PCR, and gel-purified. Electroporation was performed using the Neon Transfection System (#MPK5000) and Cas9 protein (#A36497) purchased from Thermo Fisher Scientific. Approximately 5×10^5 HeLa cells were electroporated with 25 pmol of RNPs (1:1 Cas9:gRNA ratio) and 2 µg of HDRT using the Neon Transfection System 100 µl Kit (#MPK10096) with pulse conditions of 1150 V/20 ms/2 pulses. The cells were then expanded in culture, and GFP+ cells were isolated from the mixed population at 8 d after electroporation by fluorescence-activated cell sorting. To further confirm GFP knock-in GFP-positive cells were genotyped by sequencing using oligonucleotide primer present in GFP. Additionally, cell lysates of control HeLa cells or GFP-Rab14-KI HeLa cells were incubated with GST-tagged anti-GFP nanobody-coated beads. The beads were then washed, and bound proteins were analyzed by Western blotting using anti-Rab14 antibodies (Supplemental Figure S2C).

Statistical analysis

All statistical analyses were performed using SigmaPlot or Prism softwares. All graphs show mean ± SD, unless otherwise indicated. Datasets were assessed for normal distribution using Shapiro–Wilk normality test. A *t* test was performed on all normally distributed datasets and a Mann–Whitney U test was performed for datasets that were not normally distributed. Whenever three or more groups were compared, ANOVA was used to perform statistical analysis. For multinucleation assay and time-lapse imaging, at least three randomly chosen image fields from a single coverslip were used for data collection and the experiment was then repeated three or more times (experimental replicates).

ACKNOWLEDGMENTS

We thank Jagath Junutula for Rab14 dominant-negative and constitutively active constructs. This work was supported by National Institute of Diabetes and Digestive and Kidney Diseases grant DK064380 to R.P. and National Institute of Allergy and Infectious Diseases grant 1R01AI138625 to S.V.E.

REFERENCES

Addi C, Bai J, Echard A (2018). Actin, microtubule, septin and ESCRT filament remodeling during late steps of cytokinesis. Curr Opin Cell Biol 50, 27–34.

Bai J, Wioland H, Advedissian T, Cuvelier F, Romet-Lemonne G, Echard A (2020). Actin reduction by MsrB2 is a key component of the cytokinetic abscission checkpoint and prevents tetraploidy. Proc Natl Acad Sci USA 117, 8 4169–4179.

Collins LL, Simon G, Matheson J, Wu C, Miller MC, Otani T, Yu X, Hayashi S, Prekeris R, Gould GW (2012). Rab11-FIP3 is a cell cycle-regulated phosphoprotein. BMC Cell Biol 13, 4.

Connell JW, Lindon C, Luzio JP, Reid E (2009). Spastin couples microtubule severing to membrane traffic in completion of cytokinesis and secretion. Traffic 10, 1 42–56.

Dambournet D, Machicoane M, Chesneau L, Sachse M, Rocancourt M, El Marjou A, Formstecher E, Salomon R, Goud B, Echard A (2011). Rab35 GTPase and OCRL phosphatase remodel lipids and F-actin for successful cytokinesis. Nat Cell Biol 13, 8 981–988.

Dionne LK, Wang XJ, Prekeris R (2015). Midbody: from cellular junk to regulator of cell polarity and cell fate. Curr Opin Cell Biol 35, 51–58.

Fielding AB, Schonteich E, Matheson J, Wilson G, Yu X, Hickson GR, Srivastava S, Baldwin SA, Prekeris R, Gould GW (2005). Rab11-FIP3 and FIP4 interact with Arf6 and the exocyst to control membrane traffic in cytokinesis. EMBO J 24, 19 3389–3399.

Fremont S, Echard A (2018). Membrane traffic in the late steps of cytokinesis. Curr Biol 28, 8 R458–R470.

Fremont S, Hammich H, Bai J, Wioland H, Klinkert K, Rocancourt M, Kikuti C, Stroebel D, Romet-Lemonne G, Pylypenko O, *et al.* (2017a). Oxidation of F-actin controls the terminal steps of cytokinesis. Nat Commun 8, 14528.

Fremont S, Romet-Lemonne G, Houdusse A, Echard A (2017b). Emerging roles of MICAL family proteins - from actin oxidation to membrane trafficking during cytokinesis. J Cell Sci 130, 9 1509–1517.

Gibieza P, Prekeris R (2018). Rab GTPases and cell division. Small GTPases 9, 1-2 107–115.

Guizetti J, Schermelleh L, Mantler J, Maar S, Poser I, Leonhardt H, Muller-Reichert T, Gerlich DW (2011). Cortical constriction during abscission involves helices of ESCRT-III-dependent filaments. Science 331, 6024 1616–1620.

Gundry C, Marco S, Rainero E, Miller B, Dornier E, Mitchell L, Caswell PT, Campbell AD, Hogeweg A, Sansom OJ, *et al.* (2017). Phosphorylation of Rab-coupling protein by LMTK3 controls Rab14-dependent EphA2 trafficking to promote cell:cell repulsion. Nat Commun 8, 14646.

Haeussler M, Schonig K, Eckert H, Eschstruth A, Mianne J, Renaud JB, Schneider-Maunoury S, Shkumatava A, Teboul L, Kent J, *et al.*

(2016). Evaluation of off-target and on-target scoring algorithms and integration into the guide RNA selection tool CRISPOR. Genome Biol 17, 1 148.
Hoog JL, Huisman SM, Sebo-Lemke Z, Sandblad L, McIntosh JR, Antony C, Brunner D (2011). Electron tomography reveals a flared morphology on growing microtubule ends. J Cell Sci 124(Pt 5), 693–698.
Hutagalung AH, Novick PJ (2011). Role of Rab GTPases in membrane traffic and cell physiology. Physiol Rev 91, 1 119–149.
Junutula JR, Schonteich E, Wilson GM, Peden AA, Scheller RH, Prekeris R (2004). Molecular characterization of Rab11 interactions with members of the family of Rab11-interacting proteins. J Biol Chem 279, 32 33430–33437.
Kelly EE, Horgan CP, Adams C, Patzer TM, Ni Shuilleabhain DM, Norman JC, McCaffrey MW (2009). class I Rab11-family interacting proteins are binding targets for the Rab14 GTPase. Biol Cell 102, 1 51–62.
Kouranti I, Sachse M, Arouche N, Goud B, Echard A (2006). Rab35 regulates an endocytic recycling pathway essential for the terminal steps of cytokinesis. Curr Biol 16, 17 1719–1725.
Lall P, Lindsay AJ, Hanscom S, Kecman T, Taglauer ES, McVeigh UM, Franklin E, McCaffrey MW, Khan AR (2015). Structure-function analyses of the interactions between Rab11 and Rab14 small GTPases with their shared effector Rab coupling protein (RCP). J Biol Chem 290, 30 18817–18832.
Lu R, Wilson JM (2016). Rab14 specifies the apical membrane through Arf6-mediated regulation of lipid domains and Cdc42. Sci Rep 6, 38249.
Noordstra I, Liu Q, Nijenhuis W, Hua S, Jiang K, Baars M, Remmelzwaal S, Martin M, Kapitein LC, Akhmanova A (2016). Control of apico-basal epithelial polarity by the microtubule minus-end-binding protein CAMSAP3 and spectraplakin ACF7. J Cell Sci 129, 22 4278–4288.
Pedelacq JD, Cabantous S, Tran T, Terwilliger TC, Waldo GS (2006). Engineering and characterization of a superfolder green fluorescent protein. Nat Biotechnol 24, 1 79–88.
Peden AA, Schonteich E, Chun J, Junutula JR, Scheller RH, Prekeris R (2004). The RCP-Rab11 complex regulates endocytic protein sorting. Mol Biol Cell 15, 8 3530–3541.
Peterman E, Gibieza P, Schafer J, Skeberdis VA, Kaupinis A, Valius M, Heiligenstein X, Hurbain I, Raposo G, Prekeris R (2019). The post-abscission midbody is an intracellular signaling organelle that regulates cell proliferation. Nat Commun 10, 1 3181.
Petsalaki E, Zachos G (2020). DNA damage response proteins regulating mitotic cell division: double agents preserving genome stability. Febs J 287, 1700–1721.
Prekeris R (2011). Actin regulation during abscission: unexpected roles of Rab35 and endocytic transport. Cell Res 21, 9 1283–1285.
Prekeris R (2015). Analyzing the functions of Rab11-effector proteins during cell division. Methods Cell Biol 130, 19–34.
Roth TL, Puig-Saus C, Yu R, Shifrut E, Carnevale J, Li PJ, Hiatt J, Saco J, Krystofinski P, Li H, *et al*. (2018). Reprogramming human T cell function and specificity with non-viral genome targeting. Nature 559, 7714 405–409.
Sadler JBA, Wenzel DM, Williams LK, Guindo-Martinez M, Alam SL, Mercader JM, Torrents D, Ullman KS, Sundquist WI, Martin-Serrano J (2018). A cancer-associated polymorphism in ESCRT-III disrupts the abscission checkpoint and promotes genome instability. Proc Natl Acad Sci USA 115, 38 E8900–E8.
Schiel JA, Childs C, Prekeris R (2013). Endocytic transport and cytokinesis: from regulation of the cytoskeleton to midbody inheritance. Trends Cell Biol 23, 7 319–327.
Schiel JA, Prekeris R (2010). Making the final cut - mechanisms mediating the abscission step of cytokinesis. ScientificWorldJournal 10, 1424–1434.
Schiel JA, Prekeris R (2013). Membrane dynamics during cytokinesis. Curr Opin Cell Biol 25, 1 92–98.
Schiel JA, Simon GC, Zaharris C, Weisz J, Castle D, Wu CC, Prekeris R (2012). FIP3-endosome-dependent formation of the secondary ingression mediates ESCRT-III recruitment during cytokinesis. Nat cell Biol 14, 10 1068–1078.
Simon GC, Prekeris R (2008). The role of FIP3-dependent endosome transport during cytokinesis. Commun Integr Biol 1, 2 132–133.
Simon GC, Schonteich E, Wu CC, Piekny A, Ekiert D, Yu X, Gould GW, Glotzer M, Prekeris R (2008). Sequential Cyk-4 binding to ECT2 and FIP3 regulates cleavage furrow ingression and abscission during cytokinesis. EMBO J 27, 13 1791–1803.
Sun D, Leung CL, Liem RK (2001). Characterization of the microtubule binding domain of microtubule actin crosslinking factor (MACF): identification of a novel group of microtubule associated proteins. J Cell Sci 114(Pt 1), 161–172.
Vietri M, Radulovic M, Stenmark H (2020). The many functions of ESCRTs. Nat Rev Mol Cell Biol 21, 1 25–42.
Wilson GM, Fielding AB, Simon GC, Yu X, Andrews PD, Hames RS, Frey AM, Peden AA, Gould GW, Prekeris R (2005). The FIP3-Rab11 protein complex regulates recycling endosome targeting to the cleavage furrow during late cytokinesis. Mol Biol Cell 16, 2 849–860.